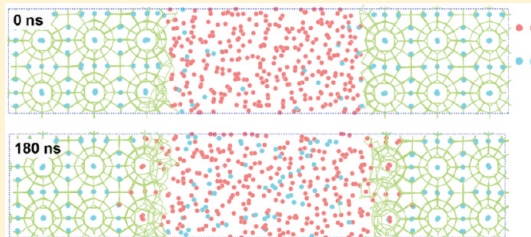


In Situ Methane Recovery and Carbon Dioxide Sequestration in Methane Hydrates: A Molecular Dynamics Simulation Study

Yen-Tien Tung, Li-Jen Chen, Yan-Ping Chen, and Shiang-Tai Lin*

Department of Chemical Engineering, National Taiwan University, Taipei 10617, Taiwan

ABSTRACT: One intriguing idea for the simultaneous recovery of energy and sequestration of global warming gas is proposed by the transformation of methane hydrates to carbon dioxide hydrates with the injection of liquid CO₂. Here we use molecular dynamics simulations to show that the replacement can take place without melting of the network of hydrogen-bonded water molecules. Depending on the distance to the interface between the liquid CO₂ and solid clathrate hydrate, we find that the replacement occurs either via direct swapping of methane and CO₂ or via a transient co-occupation of both methane and CO₂ in one cavity. Our results suggest that, with a careful design of the operation condition, it is possible to replace methane from methane hydrates with CO₂ in the solid phase without much change in the geological stability.



1. INTRODUCTION

The amount of methane entrapped in clathrate hydrate in the permafrost regions and under the deep sea-floor sediments is so abundant that it is considered as a potential new source of energy.^{1–4} Despite the economic aspects, the recovery and utilization of methane in methane hydrates (MH) has brought serious environmental concerns such as the stimulation of earthquakes, tsunamis,^{5–7} and global climate changes (e.g., global warming).¹ One intriguing idea that could resolve some of the these difficulties is to replace methane in MH with carbon dioxide by the injection of liquid CO₂ to the clathrate hydrate deposits.⁸

The conversion of MH to CO₂ hydrates has been confirmed by many experiments.^{9–16} It is found that the replacement efficiency is about 30–64%^{12,13} and the rate decays significantly with time.^{10–13} While the detailed mechanism of the replacement process is largely unknown, the data collected from lab experiments lead to the speculation of an initial decomposition of MH when brought in contact with CO₂, followed by the formation of CO₂ hydrates.^{17,18} However, the decomposition of MH would change the mechanical properties of the deposits, leading to geological instability.⁷

Molecular dynamics (MD) simulation is one powerful tool to provide molecular level understanding of microscopic mechanisms. It has been used successfully to study various aspects of clathrate hydrates, including the nucleation, growth, decomposition, and inhibition of methane and carbon dioxide hydrates.^{19–31} The purpose of the present study is to reveal the mechanism of the conversion of MH to CO₂ hydrates by performing molecular dynamics simulations. We find that the replacement can take place without melting down the network of water molecules. Depending on the distance to the interface between the liquid CO₂ and solid MH, we find that the replacement occurs either via (1) direct swapping of methane and

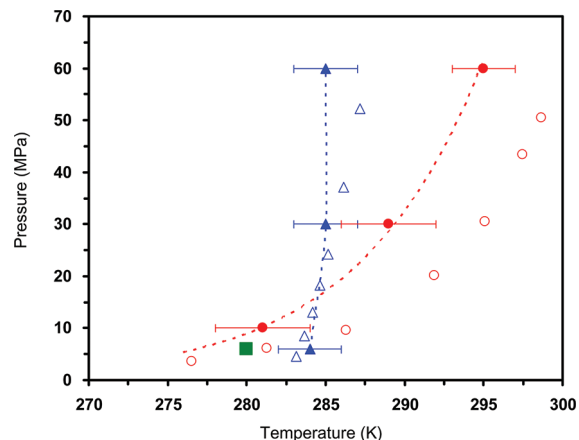


Figure 1. Three-phase coexisting condition of pure methane and pure CO₂ hydrates. Open and closed red circles represent data for methane hydrates from experiment^{37,38} and MD simulation, respectively.²⁶ Open and closed blue triangles are data for CO₂ hydrates from experiment³⁹ and MD simulation, respectively.² The green square indicates the condition used in MD simulations for the replacement of methane with CO₂.

CO₂ or via (2) a transient co-occupation of both methane and CO₂ in one cavity. Our results suggest that, with a careful design of the operation condition, it is possible to simultaneously recover methane from methane hydrates and sequester CO₂ in the solid phase without much change in the geological stability.

Received: September 14, 2011

Revised: November 7, 2011

Published: November 17, 2011

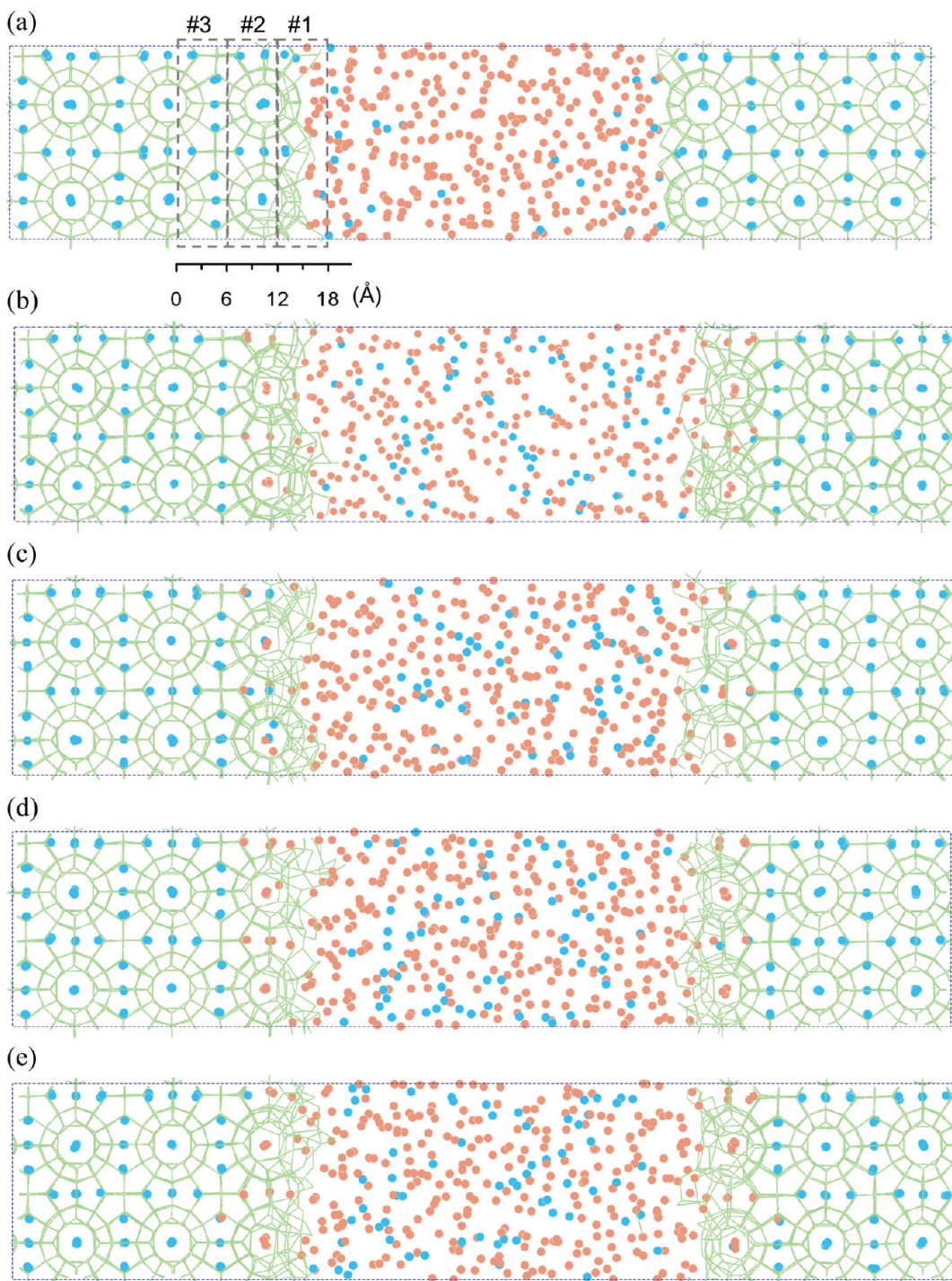


Figure 2. Snapshots taken from the MD simulation showing the replacement of methane (blue balls) in methane hydrate with liquid carbon dioxide (orange balls) at 0 (a), 10 (b), 20 (c), 40 (d), and 180 (e) ns. The green lines represent the hydrogen bonds between water molecules. The system initially (a) contains a slab of crystalline methane hydrate and a liquid CO_2 phase (in the middle). The layer ID (#1 to #3) used in the discussion is labeled in (a). Almost all the methane molecules in layer #2 are replaced by CO_2 within 20 ns (c). Some of the methane molecules are further replaced by CO_2 from 20 to 180 ns (d,e).

2. COMPUTATIONAL DETAILS

The two-phase model consisting of a CO_2 liquid and a solid methane hydrate phase is used in this study. The CO_2 phase contains 320 CO_2 molecules and the methane hydrate phase consists of a $6 \times 2 \times 2$ unit cell of structure I (sI) crystalline hydrate with all its cavities filled with methane (1104 water molecules and 204 methane molecules). The size of such an

initially created model (using molecular simulation package Cerius2³²) is $114.00 \text{ \AA} \times 23.74 \text{ \AA} \times 23.74 \text{ \AA}$. The TIP4P-Ew³³ (for water), OPLS-AA³⁴ (for methane), and EPM2³⁵ (for CO_2) force fields are chosen to describe the interactions within the molecular model. The details of interaction parameters between water and CH_4 and CO_2 can be found in previous publications.^{26,36} The equilibrium phase diagrams of CH_4 and CO_2 hydrate predicted

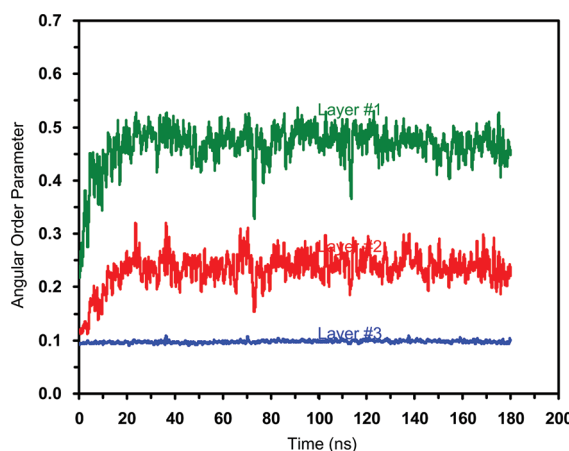


Figure 3. Time evolution of AOP of water near the solid–liquid interface. The results show that water molecules in layer #3 are hydrate-like. In layers #2 and #1 water molecules are more mobile but still quite different from the liquid water (whose AOP is 0.8).

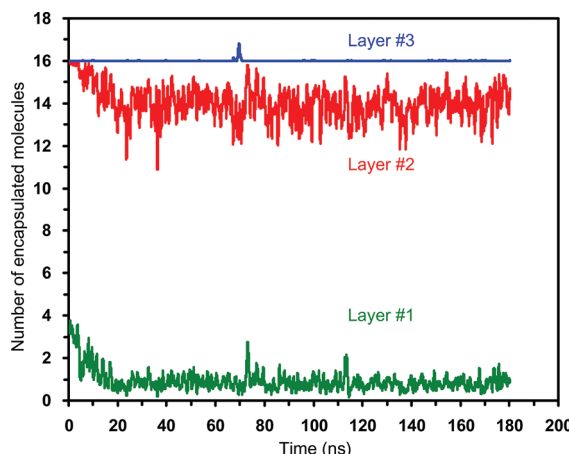


Figure 4. Time evolution of number of gas molecules (methane and CO₂) encapsulated in hydrate-like water cages. The significant fluctuation seen in layer #2 indicates soft nature of water cages in this layer, allowing swapping of methane and CO₂ molecules. The peak at around 70 ns in layer #3 indicates co-occupation of methane and CO₂ molecules in one common cage.

by using such a set of parameters were found to be in good agreement with experiment (Figure 1).^{37–39} All the molecular mechanics and dynamics simulations were performed using the open source package, LAMMPS.⁴⁰ The initially created model was energy minimized and a short, 20 ps, NVT simulation at 200 K was then performed to relax any extra stress at the solid–liquid interface. The relaxed system was then heated from 200 to 280 K at a rate of 0.5 K/ps under constant pressure of 6 MPa. Finally, the system was subjected to long (up to 180 ns) NPT simulations for the replacement of methane by CO₂. The periodic boundary condition is applied to the simulation box in all three directions. The Nose–Hoover temperature thermostat⁴¹ with a relaxation time of 0.1 ps and pressure barostat⁴² with a relaxation time of 1 ps are used. The integration time step is set to 1 fs. The Lennard-Jones potential energy is calculated with a cutoff of 9.5 Å and the long-range Coulomb energy is calculated by PPPM^{43–45} with a cutoff of 8.5 Å for the real part. To access statistics of the

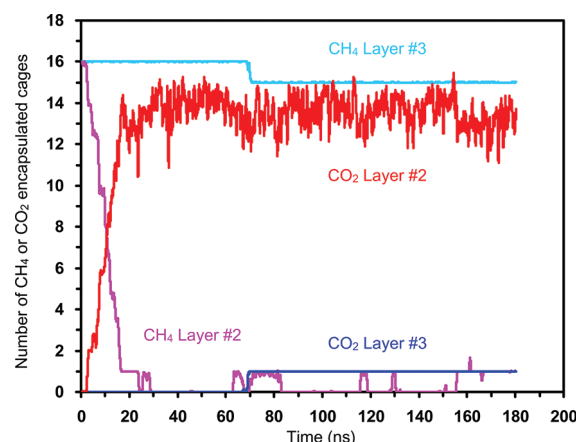


Figure 5. Time evolution of number of methane and CO₂ encapsulated cages. The nearly symmetric behavior in the change of methane and CO₂ cage numbers in layer #2 indicates swapping mechanism. The replacement of methane in layer #3 is observed at around 70 ns.

calculated properties we performed three sets of independent simulations using different random seeds for velocity initialization. We have also conducted another three independent sets of simulations using a larger system size (4 × 4 × 4 structure I (sl) crystalline hydrate and 1280 CO₂ in the liquid phase) to ensure reproducibility.

3. RESULTS AND DISCUSSION

3.1. Replacement of Methane by Carbon Dioxide. Figure 2 shows the snapshots taken from one of our molecular dynamics simulations performed under constant temperature 280 K and pressure 6 MPa. At 6 MPa, the simulation temperature is above the melting temperature of methane hydrate (277 K) and below that of CO₂ hydrate (284 K) (see Figure 1). The green lines represent hydrogen-bonded polygons (mostly pentagons and hexagons) forming the cage structure of hydrate crystal. The carbon atoms of methane and CO₂ molecules are shown in blue and orange spheres, respectively. (Other atoms are not shown for clarity.) In the beginning of the simulation, methane molecules occupy all the cages in the hydrate phase, while some located in the broken cages at the two interfaces (layer #1, see Figure 2a for the numbering of layers in the hydrate phase) dissolve to the liquid CO₂ phase. From 0 to 20 ns, methane molecules in the cages near the interface (layer #2) dissolve into the liquid phase with the CO₂ molecules simultaneously occupying the water cages. The replacement of methane with CO₂ is observed in the inner cages (layer #3) after 20 ns.

There are two distinct mechanisms of methane replacement by CO₂ depending on the rigidity of the water cages. The rigidity of cages can be measured by the angular order parameter (AOP)²⁶ of the constituting water molecules shown in Figure 3. The AOP is calculated as follows

$$\text{AOP} = \sum [(\cos \theta |\cos \theta| + \cos^2(109.47^\circ))^2] \quad (1)$$

where θ is the inclusion angle among the oxygen atom of the water molecule of interest and any two oxygen atoms of the neighboring water molecules. The summation runs over all

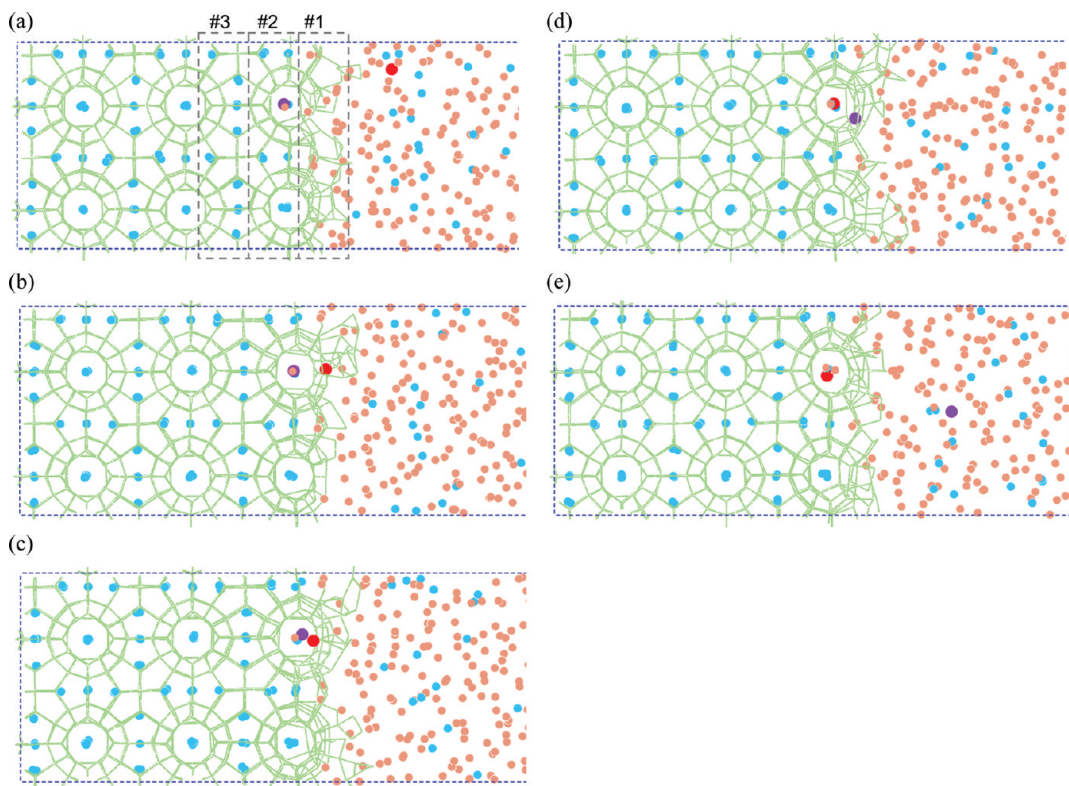


Figure 6. Snapshots (at 2.555 (a), 2.585 (b), 2.589 (c), 2.598 (d), and 2.637 (e) ns) showing the swapping of a CO₂ molecule (in red) and a methane molecule (in purple) in soft water cages (layer #2). At 2.555 ns (a), the CO₂ molecule is in the liquid phase. The position of methane and CO₂ swapped during 2.585 to 2.598 ns (b to d). The methane molecule eventually dissolves into liquid CO₂ phase (e).

possible θ of water molecules within a radius of 3.5 Å from the center oxygen atom of interest. The AOP of water in the liquid phase, clathrate hydrates, and ice are 0.8, 0.1, and 0, respectively. Therefore, the rigidity (or immobility) of water increases with a decrease of the AOP. It can be seen that water molecules at the surface layer (layer #1) possess a higher value of AOP (0.45), indicating the labile nature of these cages. Nonetheless, the AOP of water at the surface layer is significantly less than of bulk water (0.8), indicating no completely dissolved water (or liquid water film) at the interface. The AOP of water molecules in layer #3 is the same as the crystalline hydrate water (AOP value of 0.1), indicating stable and rigid cages. In between (layer #2), the water molecules show larger fluctuations from their equilibrium positions and the cages are soft. It may be worth mentioning that we did not observe a film of liquid water at the interface of liquid CO₂ and solid methane hydrate in our simulations.

Figure 4 shows the number of gas molecules (methane and CO₂ together) encapsulated by complete water cages in layers #1 to #3. There are 16 water cages in each layer of a perfect 2 × 2 structure I hydrate crystal. Since most of the cages at the surface (layer #1) are impaired (broken or incomplete), only one or two gas molecules are encapsulated by hydrate-like water. The soft nature of water cages in layer #2 can be observed from the fluctuation (11 to 16) of the number of encapsulated molecules with time. The nearly equivalent rate (slope of pink curve in Figure 5) of methane leaving layer #2 and that of CO₂ (slope of red curve in Figure 5) entering the same layer suggests that the dissolution of methane into liquid CO₂ and occupation of CO₂ into the cages occur simultaneously. As will be shown, the fluctuations of water molecules

in this layer allow for rapid swapping of CO₂ and methane molecules and the replacement reaches completion in layer #2 in about 20 ns. The high value (11 to 16) of complete water cages in layer #2 also implies that the hydrate does not melt as the replacement proceeds.

In contrast to layer #2 where a noticeable fluctuation is observed in the total number of encapsulated molecules, the number of encapsulated gas molecules in layer #3 is nearly constant but may occasionally exceed the number of water cages 16 (see Figure 4 at around 70 ns). From Figure 5 it is obvious that the excess gas molecule is caused by the entrance of CO₂ into layer #3, leading to co-occupation of CO₂ and methane in the same cage. The replacement completes as the methane molecule is expelled to layer #2. The low AOP value of water is consistent with the nearly zero fluctuation of the number of encapsulated molecules (Figure 4), indicating that the water cages in layer #3 are quite rigid.

The swapping of methane and CO₂ molecules is illustrated in Figure 6. The methane molecule (highlighted in purple) in a $5^{12}6^2$ cage in layer #2 is to be replaced by a CO₂ molecule (highlighted in red) in the liquid phase. The CO₂ molecule first enters layer #1 at 2.585 ns. At 2.589 ns, the CO₂ molecule jumps into an adjacent $5^{12}6^2$ cage in layer #2 through an opening formed by the fluctuation in the hydrogen-bonding network. The entrance of CO₂ pushes out the originally residing methane molecule to layer #1 via the same opening. The methane molecule eventually diffuses into the liquid CO₂ phase at 2.637 ns. We found that the swapping of guest molecules between layer #2 and layer #1 occurs constantly and is not limited to methane/CO₂. There are frequent

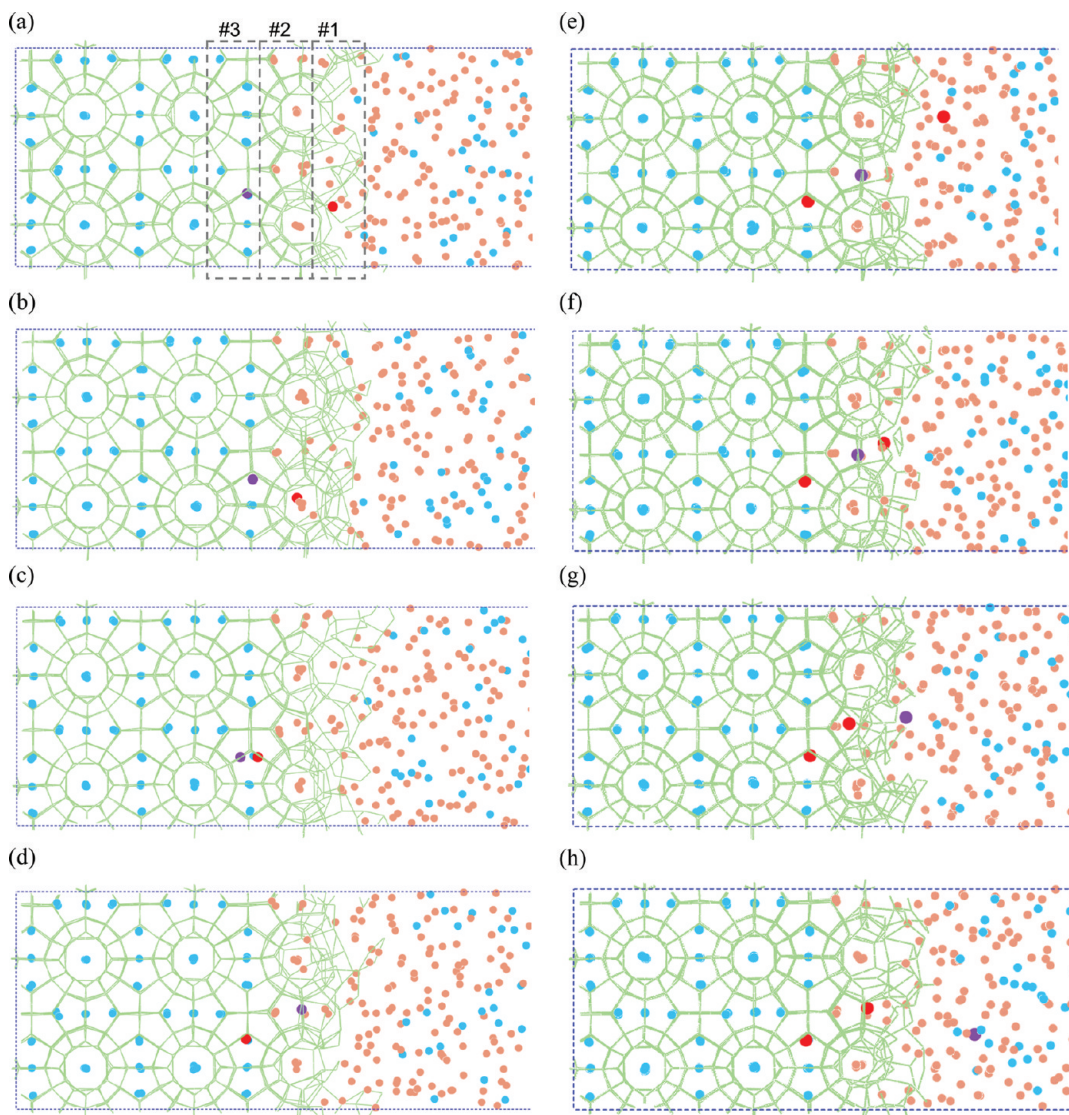


Figure 7. Snapshots (at 67.6 (a), 68.7 (b), 69.3 (c), 70.4 (d), 82.37 (e), 82.40 (f), 82.62 (g), and 85.20 (h) ns) showing the replacement of methane in rigid water cages (layer #3) via co-occupation of methane (in purple) and CO₂ (red) molecules in the same cage. At 67.6 ns (a) one CO₂ molecule in layer #1 enters a cage in layer #2 (b). At 69.3 ns (c) the CO₂ molecule enters another cage in layer #3 and stay there with a pre-existing methane molecule for about 1 ns. At 70.4 ns (d) the methane molecule is expelled to layer #2. The methane is swapped to the interface by another CO₂ molecule from the liquid phase at time 82.40 ns (f) to 82.62 ns (g). The methane molecule eventually dissolves to the liquid CO₂ phase (h).

swapping of CO₂ molecules. The constant molecular exchange via swapping allows for the occasional reoccurrence of methane (see methane reoccurrence at 62 ns and after 118 ns in Figure 5) in this layer #2.

Figure 7 illustrates the replacement of methane with CO₂ in a rigid water cage. The methane molecule highlighted in purple (layer #3) is to be replaced by a CO₂ molecule (shown as a red sphere), initially located in layer #1 (Figure 7a). At 68.7 ns (Figure 7b), this CO₂ enters into an adjacent large $S^{12}6^2$ cage in layer #2. Figure 7, b and c, shows that the CO₂ moves forward to an adjacent $S^{12}6^2$ large cage in layer #3. In contrast to swapping observed in layer #2, both the CO₂ and methane molecules are found to stay in the same cage in layer #3 for about 1–2 ns. Given the fact that the size of a $S^{12}6^2$ cage is not suitable for the co-occupation of methane and CO₂, the two molecules spin inside the cage. The spinning of molecules causes fluctuations in the hydrogen-bonding network and eventually results in an opening

that allows the escape of methane molecule to layer #2. The methane molecule is trapped in a small S^{12} cage (layer #2) for a while (Figure 7d) before it eventually dissolves into the liquid phase (Figure 7h).

Therefore, the replacement of methane with CO₂ in methane hydrate appears to be twofold. Layers right next to the surface the water cages (e.g., layer #2) are soft due to the fluctuation of water molecules, which allows for constant swapping of gas molecules. At inner layers (e.g., layer #3) both CO₂ and methane molecules coexist in the same cage before the methane molecule is repelled to liquid CO₂ phase. Our simulations suggest that the replacement may occur without melting of the hydrates. Therefore, mechanical stability in the methane hydrate deposits can be retained for in situ replacement in the ocean floor.

3.2. Cage Openings for the Passage of Gas Molecules. We observed two types of cage openings through which the CO₂

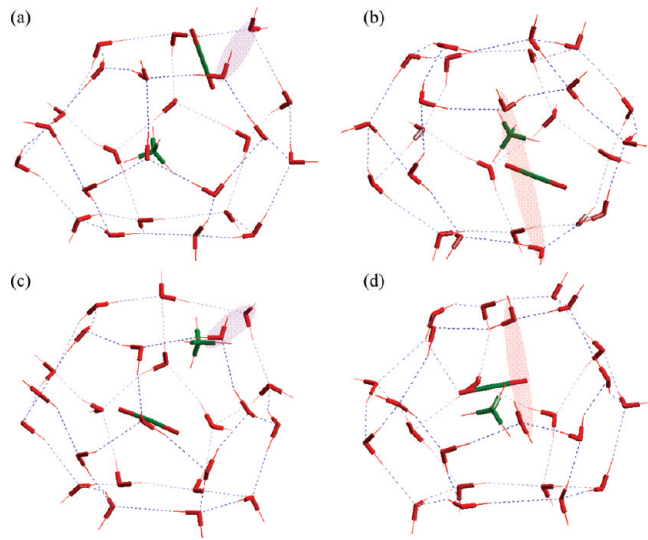


Figure 8. Two types of cage openings for the passage of CO_2 and methane. Type I: broken hydrogen bond at the junction of a hexagon and a pentagon during the passage of CO_2 (a) and methane (c). Type II: broken hydrogen bond at the junction of two pentagons during the passage of CO_2 (b) and methane (d).

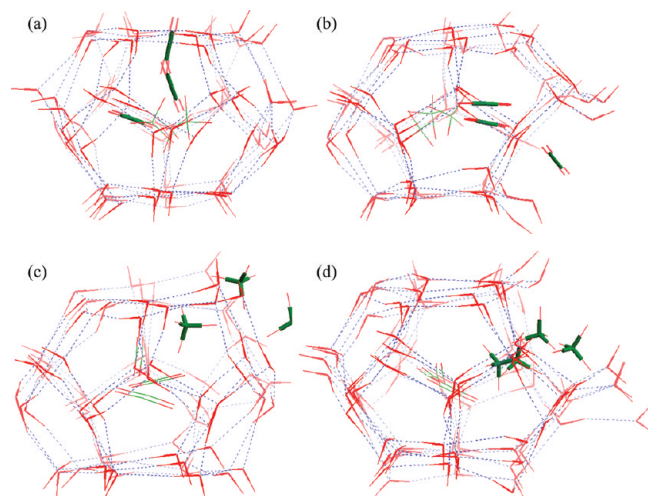


Figure 9. Illustration of the CO_2 trajectory upon the entrance to a $S^{12}6^2$ cage via type I (a) and type II (b) opening, and the trajectory of methane leaving the cage via type I (c) and type II (d) opening.

and methane may pass during the replacement process. The type I cage opening highlighted by the purple and red regions in Figure 8a is found to be located at the hydrogen-bonded junction with the hexagon and the pentagon of the large hexagonal truncated trapezohedron $S^{12}6^2$ cage. The type II cage opening highlighted by the two red regions in Figure 8b is found to be located at the hydrogen-bonded junction with the two adjacent pentagons of the large hexagonal truncated trapezohedron $S^{12}6^2$ cage. In both cases, the cage opening is caused by breaking of a hydrogen bond between water molecules constituting the polygons of cage. Figure 8, c and d, shows these two types of cage openings while the methane passes through during the replacement. It is also clearly shown that the carbon dioxide and methane (two different

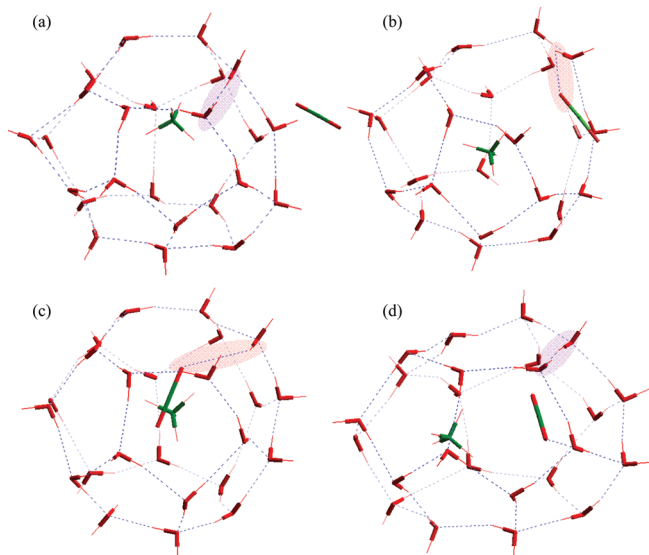


Figure 10. Opening of a $S^{12}6^2$ cage via hydrogen-bonding interaction between water and CO_2 molecules. The approach of the CO_2 molecule attracts the cage water molecule to reorient its hydrogen bond (a), which leads to an opening that allows the CO_2 molecule to enter (b,c). The re-formation of the water hydrogen bond after the entrance of CO_2 (d).

types of guest molecules) occupy the one cage as we discussed previously. Figure 9 shows the trajectories of the process where carbon dioxide enters and methane molecules leaves the cages through the type I and II of openings, respectively.

In most cases of our simulations, the openings are usually caused by the fluctuation of cage water molecules. However, there are a few cases where the openings are created by the hydrogen bonding between the oxygen atoms of water and carbon dioxide molecule entering into the cage. Figure 10 shows how the opening is formed by the hydrogen bonding between the oxygen atoms of water and carbon dioxide molecule. The newly formed hydrogen bond between the CO_2 and water also pulls the CO_2 molecule into the cage. In addition, it is also interesting to note that methane would expand the opening when it passes through due to its strong hydrophobicity (can be seen in Figure 9b as well).

The dynamic evolution of the open and close of the cage depends on the location of the broken hydrogen bond. Figure 11a shows the evolution of cage structure in the case where the carbon dioxide enters into the $S^{12}6^2$ cage through a type I opening. It is clearly shown that, after the carbon dioxide enters into the $S^{12}6^2$ cage, the opening is closed immediately by the hydrogen bonding between the original pentagon and hexagon. Figures 11b and c show the time evolution of polygons constituting the cage before and after the carbon dioxide entering into the $S^{12}6^2$ cage via a type II opening. In this case, transient polygons (hexagons or rectangles) would form after the carbon dioxide passes through the opening. The opening area is filled with additional transient polygons (hexagons or rectangles) and eventually with the pentagon to form the thermodynamically stable $S^{12}6^2$ cage structure. In other words, type I opening is closed immediately while the type II opening is filled with additional transient polygons before eventual formation of the correct pentagon of the $S^{12}6^2$ cage.

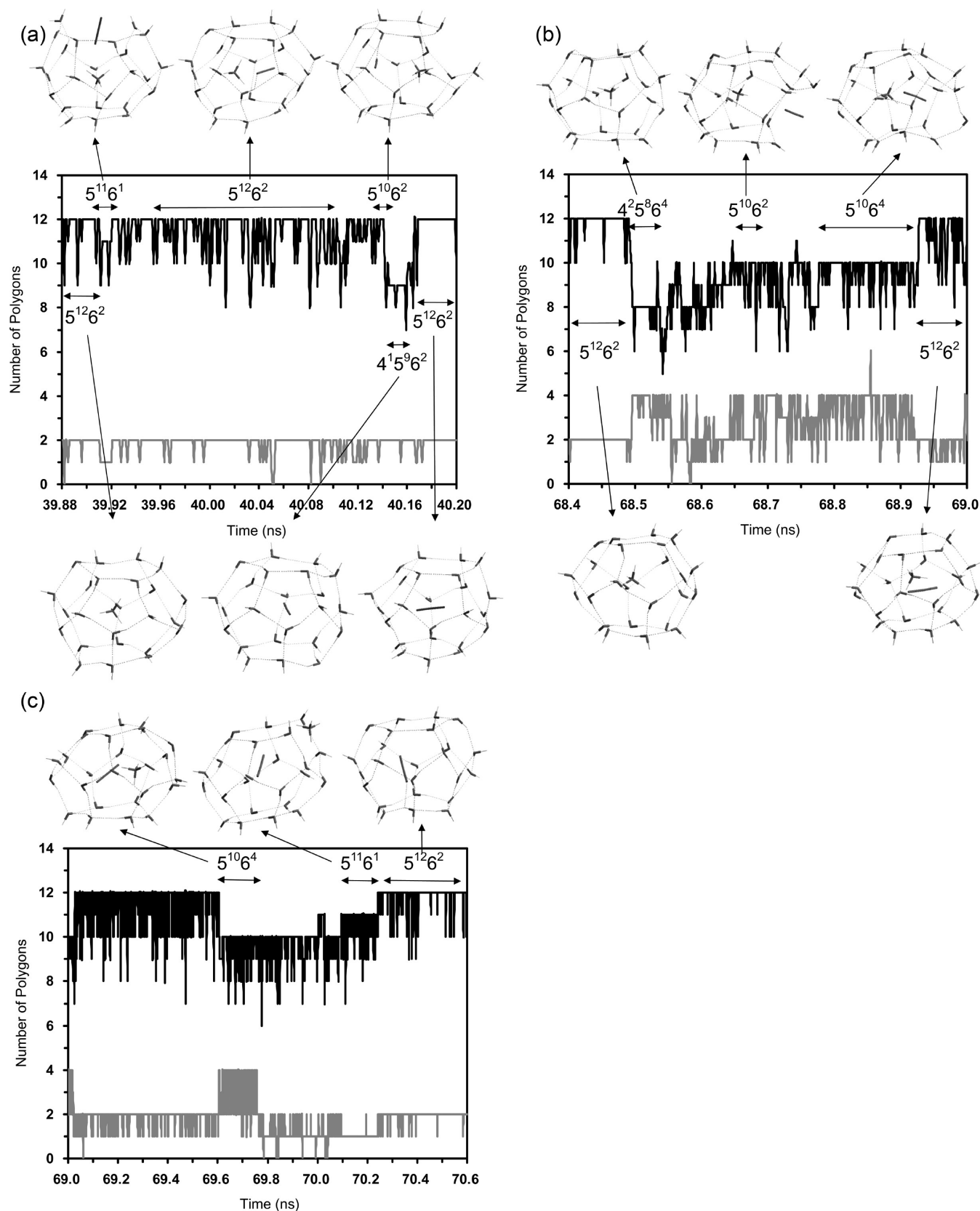


Figure 11. Time evolution of polygons (black line, pentagon; gray line, hexagon) of a $5^{12}6^2$ cage upon the entrance of a CO_2 molecule and the exit of a methane molecule. The CO_2 molecule enters the cage through a type I opening (a) or a type II opening (b, c). The originally residing methane molecule may coexist with CO_2 in the same cage for up to 2 ns before it is expelled. The analysis also reveals many nonstandard cage structures that appear during the replacement process.

4. CONCLUSION

By use of molecular dynamics simulations, the microscopic mechanism of spontaneous carbon dioxide replacement of methane in the cage of clathrate hydrate is unveiled. It is shown that the replacement can take place without melting down of water molecules network. Therefore, it is possible to recover methane from methane hydrates using liquid CO₂ in a way without causing a large-scale landslides, earthquakes, and/or tsunami. It may be worth pointing out that the present work does not address other important issues such as the rate of such replacement processes and the possible effects from the dissipation of heat during the replacement process.

We found two distinct mechanisms of methane replacement by CO₂ depending on the rigidity of the water cages. Near the surface of the methane hydrates the water cages are soft (hydrogen bonds break and re-form due to fluctuations), and the replacement occurs via direct swapping of methane and CO₂. At layers away from the solid hydrate surface the water cages are rigid, and the replacement occurs through a transient co-occupation of both methane and CO₂ in one cavity.

We found two types of cage opening through which a carbon dioxide/methane molecule enters into/leaves the cage during the replacement. The type I and II openings are identified to be located at the hydrogen-bonded junction with the hexagon and the pentagon and two adjacent pentagons, respectively, of the large hexagonal truncated trapezohedron 5¹²6² cage. The passage of a molecule through different types of opening leads to remarkably distinct cage re-forms to close the opening. The broken hydrogen bond in the type I opening is found to re-form immediately after the passage of the gas molecule. However, the water molecules involved in the broken hydrogen bond of a type II opening can easily form hydrogen bonds with nearby water molecules, leading to the formation of transient rectangles and hexagons before the reformation of the proper pentagon of the 5¹²6² cage.

AUTHOR INFORMATION

Corresponding Author

*E-mail: stlin@ntu.edu.tw.

ACKNOWLEDGMENT

The authors are thankful for the financial support through grants 100-5226904000-04-04 and 99-5226904000-04-04 by the Ministry of Economic Affairs of Taiwan, NSC 98-2221-E-002-087-MY3 by the National Science Council of Taiwan, and computation resources from the National Center for High-Performance Computing of Taiwan and Computer and Information Networking Center of National Taiwan University.

REFERENCES

- (1) Kvenvolden, K. A. *Rev. Geophys.* **1993**, *31*, 173.
- (2) Gornitz, V.; Fung, I. *Global Biogeochem. Cycles* **1994**, *8*, 335.
- (3) Dickens, G. R.; Paull, C. K.; Wallace, P. *Nature* **1997**, *385*, 426.
- (4) Haq, B. U. *Science* **1999**, *285*, 543.
- (5) Lopez, C.; Spence, G.; Hyndman, R.; Kelley, D. *Geology* **2010**, *38*, 967.
- (6) Sultan, N.; Cochonat, P.; Canals, M.; Cattaneo, A.; Dennielou, B.; Hafidason, H.; Laberg, J. S.; Long, D.; Mienert, J.; Trincardi, F.; Urgeles, R.; Vorren, T. O.; Wilson, C. *Marine Geol.* **2004**, *213*, 291.
- (7) Pearce, F. *New Scientist* **2009**, *202*, 30.
- (8) Ohgaki, K.; Takano, K.; Sangawa, H.; Matsubara, T.; Nakano, S. *J. Chem. Eng. Jpn.* **1996**, *29*, 478.
- (9) Ohgaki, K.; Takano, K.; Moritoki, M. *Kagaku Kogaku Ronbunshu* **1994**, *20*, 121.
- (10) Lee, H.; Seo, Y.; Seo, Y. T.; Moudrakovski, I. L.; Ripmeester, J. A. *Angew. Chem., Int. Ed.* **2003**, *42*, 5048.
- (11) Yoon, J. H.; Kawamura, T.; Yamamoto, Y.; Komai, T. *J. Phys. Chem. A* **2004**, *108*, 5057.
- (12) Park, Y.; Kim, D. Y.; Lee, J. W.; Huh, D. G.; Park, K. P.; Lee, J.; Lee, H. *Proc. Natl. Acad. Sci. U.S.A.* **2006**, *103*, 12690.
- (13) Ota, M.; Saito, T.; Aida, T.; Watanabe, M.; Sato, Y.; Smith, R. L.; Inomata, H. *AIChE J.* **2007**, *53*, 271S.
- (14) Tegze, G.; Granasy, L.; Kvamme, B. *Phys. Chem. Chem. Phys.* **2007**, *9*, 3104.
- (15) Zhou, X. T.; Fan, S. S.; Liang, D. Q.; Du, J. W. *Energy Convers. Manage.* **2008**, *49*, 2124.
- (16) Jung, J. W.; Espinoza, D. N.; Santamarina, J. C. *J. Geophys. Res.—Solid Earth* **2010**, *115*, B10102.
- (17) Ota, M.; Abe, Y.; Watanabe, M.; Smith, R. L.; Inomata, H. *Fluid Phase Equilib.* **2005**, *228*, 553.
- (18) Ota, M.; Morohashi, K.; Abe, Y.; Watanabe, M.; Smith, R. L.; Inomata, H. *Energy Convers. Manage.* **2005**, *46*, 1680.
- (19) Moon, C.; Taylor, P. C.; Rodger, P. M. *J. Am. Chem. Soc.* **2003**, *125*, 4706.
- (20) Anderson, B. J.; Tester, J. W.; Borghi, G. P.; Trout, B. L. *J. Am. Chem. Soc.* **2005**, *127*, 17852.
- (21) Vatamanu, J.; Kusalik, P. G. *J. Am. Chem. Soc.* **2006**, *128*, 15588.
- (22) English, N. J.; Phelan, G. M. *J. Chem. Phys.* **2009**, *131*, 074704.
- (23) Walsh, M. R.; Koh, C. A.; Sloan, E. D.; Sum, A. K.; Wu, D. T. *Science* **2009**, *326*, 1095.
- (24) Geng, C. Y.; Wen, H.; Zhou, H. *J. Phys. Chem. A* **2009**, *113*, 5463.
- (25) Tung, Y. T.; Chen, L. J.; Chen, Y. P.; Lin, S. T. *J. Phys. Chem. C* **2011**, *115*, 7504.
- (26) Tung, Y. T.; Chen, L. J.; Chen, Y. P.; Lin, S. T. *J. Phys. Chem. B* **2010**, *114*, 10804.
- (27) Vatamanu, J.; Kusalik, P. G. *J. Phys. Chem. B* **2008**, *112*, 2399.
- (28) Hawtin, R. W.; Quigley, D.; Rodger, P. M. *Phys. Chem. Chem. Phys.* **2008**, *10*, 4853.
- (29) Zhang, J. F.; Hawtin, R. W.; Yang, Y.; Nakagava, E.; Rivero, M.; Choi, S. K.; Rodger, P. M. *J. Phys. Chem. B* **2008**, *112*, 10608.
- (30) Jacobson, L. C.; Hujo, W.; Molinero, V. *J. Phys. Chem. B* **2010**, *114*, 13796.
- (31) Vatamanu, J.; Kusalik, P. G. *Phys. Chem. Chem. Phys.* **2010**, *12*, 15065.
- (32) Cerius2; Molecular Simulations Inc.: San Diego, CA, 1999.
- (33) Jorgensen, W. L.; Chandrasekhar, J.; Madura, J. D.; Impey, R. W.; Klein, M. L. *J. Chem. Phys.* **1983**, *79*, 926.
- (34) Jorgensen, W. L.; Maxwell, D. S.; TiradoRives, J. *J. Am. Chem. Soc.* **1996**, *118*, 11225.
- (35) Harris, J. G.; Yung, K. H. *J. Phys. Chem.* **1995**, *99*, 12021.
- (36) Tung, Y. T.; Chen, L. J.; Chen, Y. P.; Lin, S. T. *J. Phys. Chem. C* **2011**, *115*, 7504.
- (37) Yang, S. O.; Cho, S. H.; Lee, H.; Lee, C. S. *Fluid Phase Equilib.* **2001**, *185*, 53.
- (38) Jager, M. D.; Sloan, E. D. *Fluid Phase Equilib.* **2001**, *185*, 89.
- (39) Takenouchi, S.; Kennedy, G. C. *J. Geol.* **1965**, *73*, 383.
- (40) Plimpton, S. *J. Comput. Phys.* **1995**, *117*, 1.
- (41) Hoover, W. G. *Phys. Rev. A* **1985**, *31*, 1695.
- (42) Hoover, W. G. *Phys. Rev. A* **1986**, *34*, 2499.
- (43) Darden, T.; York, D.; Pedersen, L. *J. Chem. Phys.* **1993**, *98*, 10089.
- (44) Hockney, R. W.; Eastwood, J. W. *Computer Simulation Using Particles*; Adam Hilger: New York, 1989.
- (45) Pollock, E. L.; Glosli, J. *Comput. Phys. Commun.* **1996**, *95*, 93.